Acta Cryst. (1953). **6**, 638

The Hypothesis of Parallel Rod-like Polypeptide Chains in Horse Hemoglobin*

By Dorothy Wrinch

Department of Physics, Smith College, Northampton, Mass., U.S.A.

(*Received* 19 *November* 1952)

In the discussion of his three-dimensional vector map for the monoclinic horse methemoglobin crystal No. 5, Perutz made the first claim ever made that there are rod-like structures in the vector maps of protein crystals. He also suggested a certain set of parallel rod-like polypeptide chains as the structure of horse hemoglobin. In 1952, three years later, a rather different set of parallel rod-like polypeptide chains was claimed as the structure of horse hemoglobin by Bragg, Howells & Perutz, the X-ray data studied being confined to (0*kl*) intensities of relatively long spacings obtained from three monoclinic horse hemoglobin hydrates, including crystal No. 5. It is the purpose of this communication to study Perutz's claim and the Bragg–Howells–Perutz structure and similar structures in the light of all the published vector maps of the monoclinic horse methemoglobin hydrates, including the three-dimensional vector map for crystal No. 5. From the study, it is concluded that the vector rods claimed by Perutz do not, in fact, exist. It is further concluded that there are, in these vector maps, indications that the horse hemoglobin entity does not have the Bragg–Howells–Perutz structure or, indeed, any structure comprising a set of parallel rod-like polypeptide chains.

1. Introduction

In 1949 Perutz (1949) claimed that there exists, in his three-dimensional vector map of horse methemoglobin, a set of parallel rod-like structures ('vector rods') in virtue of which the presence, in the crystal, of sets of parallel rod-like polypeptide chains constituting the hemoglobin entities may be asserted. He also proposed a particular arrangement of polypeptide chains in parallel, with a 5 Å repeat along their lengths, as the structure of hemoglobin. Later, Bragg, Howells & Perutz (1952) formulated a rather different set of parallel rod-like polypeptide chains, also with a 5 Å repeat along their lengths, for the hemoglobin structure. It is the purpose of this communication to examine (1) Perutz's claim, (2) the Bragg–Howells–Perutz structure, and (3) similar structures, with or without 5 Å repeats, in the light of the published projections and sections of the vector maps of the monoclinic horse methemoglobin hydrates.

The horse methemoglobin crystal 'normal wet', upon which the major part of the experimental work was done, is monoclinic, with space group $C2$ and $a = 109$, $b = 63{\cdot}2$, $c = 54{\cdot}4$ Å, $\beta = 111°$. In both hypotheses which have been formulated regarding the hemoglobin structure, the chains are set in the a-direction. Bragg *et al.* (1952) suggested the molecular pattern shown in Fig. 1(*a*) with the chains set on five 'layers' of a hexagonal network of metric $b/6$. The molecular pattern suggested by Perutz (1949) in the earlier paper comprised a four-layer pattern of somewhat the same type.

(*a*) We may begin by studying the more recently

* This work is supported by the Office of Naval Research.

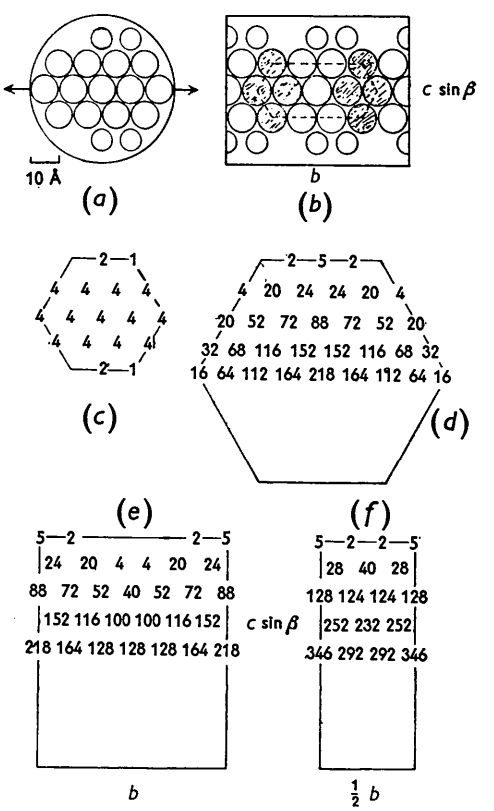

Fig. 1. (*a*) and (*b*), reproduced from Bragg *et al.* (1952), show the suggested placing of rod-like polypeptide chains in the a direction, for a single hemoglobin entity and for the unit cell respectively. (*c*) shows the relative weights assigned to the various chains and (*d*) the vector map of this set of weighted points. (*e*) allows for the overlap of the vector maps for lattice points 0, 0, 0; 0, 1, 0; etc. and (*f*) for the overlap for lattice points 0, 0, 0; ½, ½, 0; 0, 1, 0; etc.

formulated molecular pattern of parallel rods shown in Fig. 1(*a*) and (*b*). In Fig. 1(*d*) we depict the vector map of these five 'layers' of chains projected normal to their length as there shown, following Bragg *et al.* in treating them as 'point scatterers of weights 1, $\frac{1}{2}$ and $\frac{1}{4}$' multiplying all the 'weights' by 4 for convenience. These 'point scatterers' lie on the hexagonal network defined by the points $y = 0$ and $b/6$, $z' = 0$; $y = b/12$, $z' = b\sqrt{3}/12$. The vector map comprises a set of points of various weights on the same hexagonal network, now extended to cover the nine layers indicated in Fig. 1(*d*), which we may designate as $0, \pm1, \pm2, \pm3, \pm4$. Taking into account the overlapping of vector maps at lattice points 0, 0, 0; 0, 1, 0; etc. and 0, 0, 0; $\frac{1}{2}, \frac{1}{2}, 0$; 0, 1, 0; etc., the weights are as shown in Fig. 1(*e*) and (*f*) respectively. Overlapping from neighboring lattice points in the direction normal to b introduces a different hexagonal network: $b\sqrt{3}/12$ is equal not to an aliquot part of $c \sin \beta$ but to $0{\cdot}18c \sin \beta$ and the layer +4 from one set lies *between* the layers −1 and −2 of the next, the layer +3 *between* the layers −2 and −3 and the layer +2 *between* the layers −3 and −4. However, in the sequel we shall consider only the entries in the five central layers, $0, \pm1, \pm2$, since the entries in the layers ±3 and ±4 are relatively small and amount altogether to less than 6% of the total of all the entries.

We may, further, visualize the three-dimensional vector map, if we can visualize the vector map of a single one of the chains, all of which are presumably being taken as identical apart from their different 'weights'. This is a complicated matter, since the structure of the vector rod depends upon the atomic pattern of the chain and, in particular, on the specification of a 5 Å repeat along its length. However, assuming simply a 'rod-like' chain, this structure will have a rod-like periphery of double its dimensions. With the chains assumed to be of length 60–70 Å, the 'vector rods' will be of length 120–140 Å: since $a = 109$ Å, they will overlap and extend throughout the crystal in the a-direction.

Now that we have an outline picture of the set of variously weighted 'vector rods' in parallel which emerges from the proposed structure in Fig. 1(*a*), we are ready to test the structure by comparing this 'synthetic' vector map with the 'experimental' vector-map projections and sections obtained by computation from observed intensities.

(*b*) Before doing this we may turn to the earlier paper, by Perutz (1949) alone. In this paper, formulating a different molecular pattern of rod-like polypeptides parallel to the a-axis (presumably now superseded by the pattern just discussed), the main point of interest today is Perutz's claim that there exists in the experimental vector map the set of vector rods which, somewhat 'idealized', is shown in Fig. 2. These rods, we gather from the discussion (Perutz, 1949, pp. 485–6), have their axes along the lines $y = 0$, $z = 0$; $y = \pm7b/60$, $z = \pm c/6$; $y = \pm b/6$, $z = 0$.

We remark that, in this set, three of the seven vector rods lie on vector rods shown in Fig. 1 derived from the Bragg–Howells–Perutz structure, while the remaining four are somewhat displaced from rods in

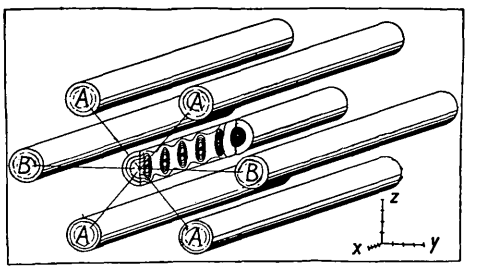

Fig. 2. An 'idealized' picture of the set of vector rods which Perutz claims is present in his three-dimensional vector map of the horse methemoglobin crystal No. 5. (This figure is reproduced by permission of the Royal Society from Perutz (1949); the scale marks on the axial cross give Ångström units).

this figure, with $y = \pm7b/60$, $z' = \pm c \sin \beta/6$ in place of $y = \pm5b/60$, $z' = \pm0{\cdot}18c \sin \beta$. Thus the set of vector rods in Fig. 2, whose presence was claimed by Perutz in 1949, is not identical with, and is not, indeed, a subset of, the vector rods in Fig. 1(*d*) whose presence is required by the structure proposed by Bragg *et al.* in 1952. The claim made in 1949 and the structure proposed in 1952 cannot both be correct.

In the sequel, the evidence as to the presence or absence of this (*b*) set of seven vector rods in the experimental vector maps will be examined, side by side with the examination of the presence or absence of the (*a*) set of vector rods depicted in Fig. 1(*d*).

Quite apart from difficult questions as to the correlation of the proposed set of rods in the actual crystal with this set of seven vector rods, this claim is of very considerable importance. It marked the first time that a claim had ever been made that there are in fact any vector rods in the vector map of any protein crystal. The careful examination of the arguments by which Perutz seeks to establish his claim thus constitutes an important part of the present investigation.

Regarding the presence or absence of the set of vector rods (*a*), there is no discussion in the literature. The only X-ray data cited by Bragg *et al.* in support of their structure are the (0*kl*) intensities of relatively long spacings obtained by Boyes-Watson *et al.* (1947) from three of the monoclinic horse methemoglobin hydrates. However, the paper is prefaced by the statement that the analysis 'is based on the assumption that the protein molecule consists for the greater part of parallel polypeptide chains in a hexagonal packing with an inter-chain distance of 10·5 Å', the only remaining questions with this viewpoint being which particular set of chains on this network should be selected and what their atomic configurations should be. Further, it is stated later that the structure pro-

posed is based 'on the chain interpretation of the Patterson diagrams, and is of significance only if it is correct'. In discussing the evidence regarding the existence in the vector map of the (*a*) set of vector rods, emerging from this structure, we can thus test the assumptions upon which the paper by Bragg *et al.* is based.

2. Vector projections

We begin by studying the projections of the two arrays of vector rods on the three vector projections calculated from observed intensities which were recorded by Boyes-Watson, Davidson & Perutz (1947). In Fig. 3, all three projections are given, as in Fig. 3 of that paper. It is apparent that, on the basis of either set of vector rods, there should be a qualitative difference between the *a*-projection and the *b*- and *c*-projections.

On the *a*-projection, small circles (confined to half the map so as to leave the other half in its original form) indicate the points into which the axes of the (*a*) set of rods project. We can also visualize the single hexagon of points into which the axes of the (*b*) set project. We remark the approach to the $b/6$ hexagonal network of the high density regions over most of the map. But the point $y = b/6$, $z' = 0{\cdot}36c \sin\beta$ of the (*a*) set misses the nearby peak (which is thus left unaccounted for) and there is little indication of the ratio of weights shown in the entries in Fig. 1(*f*).

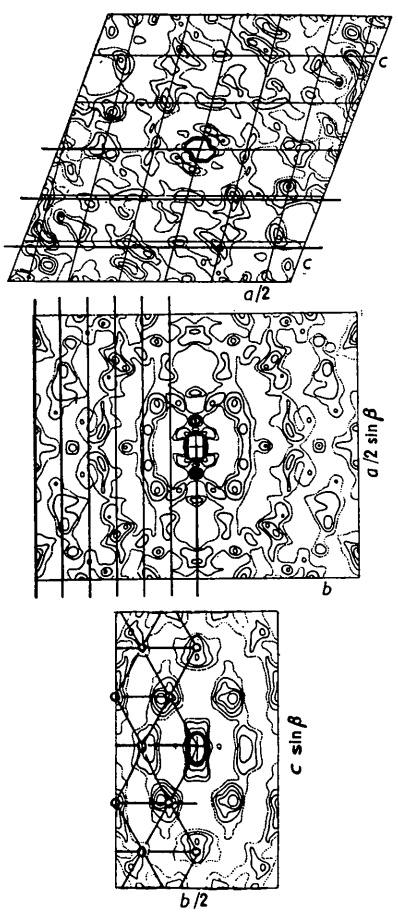

Fig. 3. Three vector projections of the horse methemoglobin crystal No. 5, reproduced by permission of the Royal Society from Boyes-Watson *et al.* (1947), on which lines and small circles have been drawn to show where the axes of the five central 'layers' of vector rods shown in Fig. 1(*f*) lie.

On the *b*-projection, the axes of the (*a*) set of vector rods project into lines parallel to *a* at $z/c = 0, \pm 0{\cdot}18, \pm 0{\cdot}36$, as indicated by the darker lines overlapping the cell boundaries shown over half the map. For the (*b*) set we would have the lines at $z/c = 0, \pm 1/6$. But there is no indication of the vector rods about any of these lines. The distribution of 'peaks' lacks any uniaxial character in the *a*-direction, or indeed in any direction. On the contrary, the distribution of high-density regions is closely associated with the nodes of a certain lattice. This fact, first pointed out by Crowfoot (1941), was stressed by Boyes-Watson *et al.* (1947), who emphasized it by actually drawing the lattice seen on the map. Particularly interesting in connection with this essentially two-dimensional and definitely not uniaxial distribution of high-density regions is the distribution of 'peaks' nearest the origin. We remark no less than three pairs of 'peaks' at about 5 Å from the origin. These are in widely different directions from the origin, being approximately in a hexagonal arrangement. While the evidence against vector rods is already clear and unambiguous in this map, it is nevertheless interesting to notice (1) that none of these 5 Å peaks lies in the *a*-direction from the origin, where the 5 Å repeat along the chains might be expected to manifest itself most strongly, and (2) that chains with the 5 Å repeat along the *a*-direction would not produce 5 Å peaks in other directions.

Looking now at the third projection, the *c*-projection, we see the lines $12y/b = 0, 1, \ldots, 6$ into which the axes of the foreshortened rods of the (*a*) set project, and we can visualize the lines for the (*b*) set. Again we reach the same conclusion. It is evident that this vector map lacks any uniaxial character in the $a \sin\beta$ direction or in any direction, as was indeed earlier recognized by Boyes-Watson *et al.* (1947) in their statement that 'the most prominent features of the *c*-projection are two rings of peaks at 10–11 and 20–22 Å from the origin'.

To sum up the situation, we may notice that the expected qualitative difference, between the *a*-projection on the one hand and the *b*- and *c*-projections on the other, has not materialized. Studying the halves of the maps left in the original state, our impression is rather of a general resemblance between all three. We can only conclude that, so far as these projections are concerned, evidence which might have been expected if the structure proposed by Bragg *et al.* is correct, is lacking. We also have to conclude that there is no evidence in these projections of the vector rods pictured in Fig. 2. If we re-read the argument, we see that a far wider statement on the same lines can be

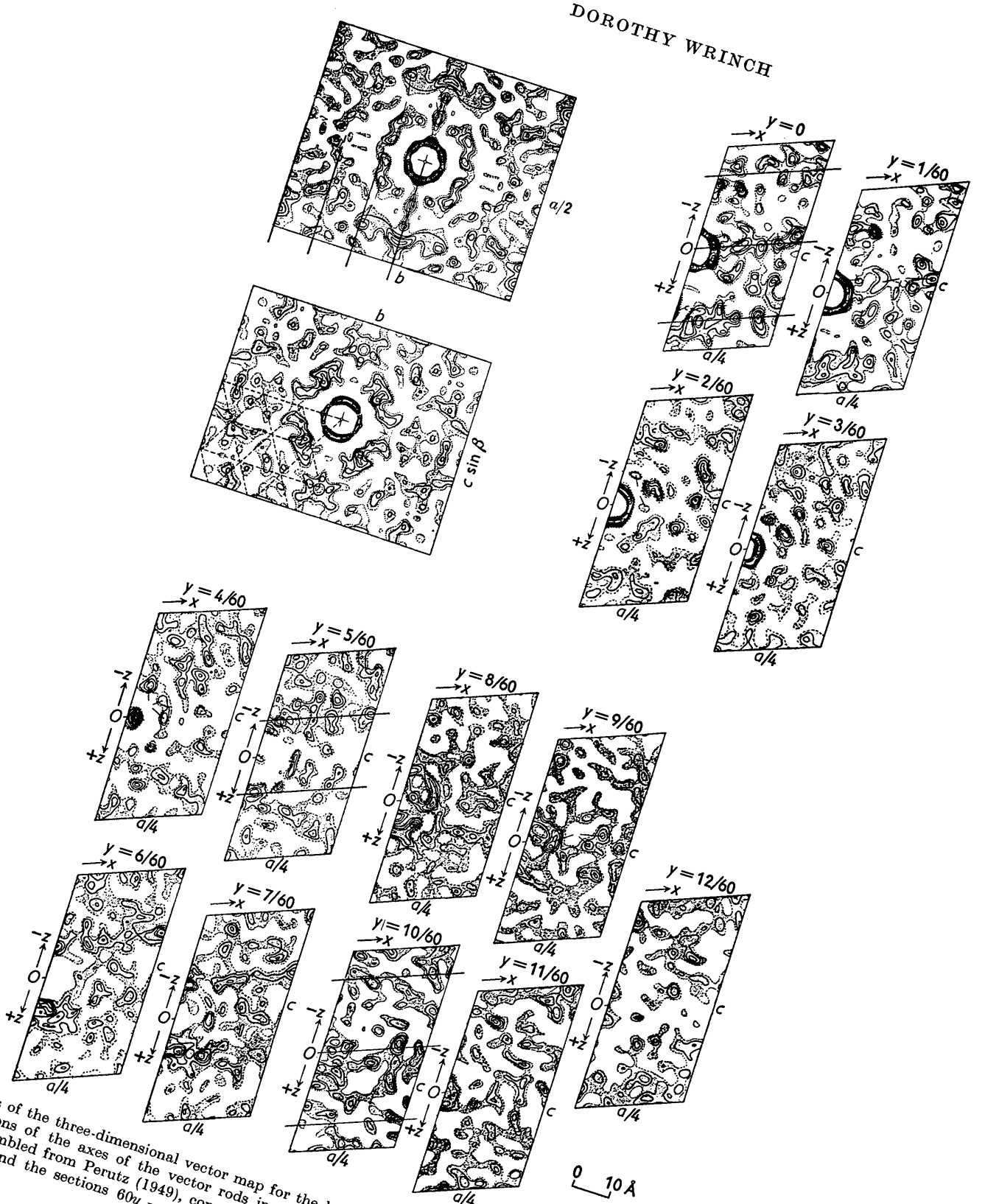

Fig. 4. The sections of the three-dimensional vector map for the horse methemoglobin crystal No. 5 published by Perutz, on which the positions of the axes of the vector rods in the five central 'layers' shown in Fig. 1(*e*) have been indicated. The sections, assembled from Perutz (1949), comprise his central sections normal to the *a* axis and containing the *a* and *b* axes (upper left) and the sections $60y = 0, 1, \ldots 12$. (Reproduced by permission of the Royal Society.)

made. Evidence which would be expected for any set of parallel rod-like polypeptide chains in any direction in the hemoglobin crystal has failed to materialize. There are, in fact, no indications of the presence of 'vector rods'.

However, it is not necessary to rely exclusively on the evidence of these three projections. It is a striking feature of Perutz's long-term X-ray studies of horse hemoglobin that no less than twelve hydrates of this protein were studied (Boyes-Watson *et al.*, 1947). Of these twelve crystals, ten are monoclinic. And of the ten, five crystals, Nos. 3–7 have the same a and b parameters; and of these five, the 'normal wet' crystal is No. 5.

In Fig. 4 of their paper Boyes-Watson *et al.* (1947) record the vector projections along the dyad axis for the sequence of crystals 3–7 superimposed two at a time. In each case we see that there are peaks at about 5 Å from the origin, though never in the a-direction. Further, there is still no sign of the uniaxial distributions of vector density expected for either the (a) or (b) set of vector rods. Indeed, the superpositions of the maps focuses attention, even more strikingly than the earlier figures, on the general characteristic of all the vector projections so far studied, the fact that there are high-density regions at about 9–11 Å disposed around the origin in every case, as Boyes-Watson *et al.* (1947) remarked. The conclusion seems inescapable: whatever the nature of the structures in the horse methemoglobin crystal may be, it must be such as to explain (1) the 5 Å peaks in various directions (not the a-direction) in the b-projections, and (2) the existence of high-density regions at say 9–11 Å from the origin in many different directions, for projections of the normal wet crystal in the a-direction and in the c-direction, and now for projections of all five hydrates in the b-direction. That no set of rod-like structures in the a-direction, normal to the b axis, can provide an explanation of either of these features in the case of any of the set of b-projections seems clear.

3. The three-dimensional vector map

We have already, in Fig. 3, reproduced some of the vector projections which have been published for horse methemoglobin, but the major part of the 'vector' evidence available regarding the structure of methemoglobin still remains to be discussed. In 1949, Perutz (1949) published certain sections of the three-dimensional vector distribution for the normal wet No. 5 crystal, and in fact, used this map in advancing his claim that the vector rods in Fig. 2 are present. Deduced by computation from some 7000 independent relative intensities, this vector map represents the most detailed data regarding any crystalline protein ever obtained.

In Figs. 4 and 5 all the published sections of this three-dimensional map are shown.* In Fig. 4, the complete central sections normal to a and containing the a and b axes and 13 of the 31 half-sections normal to the dyad axis, namely the sections $60y/b = 0, 1, \ldots 12$ for $x = 0$ to $\frac{1}{4}a$, given by Perutz (1949), have been assembled. In Fig. 5 we add the complete $y = 0$

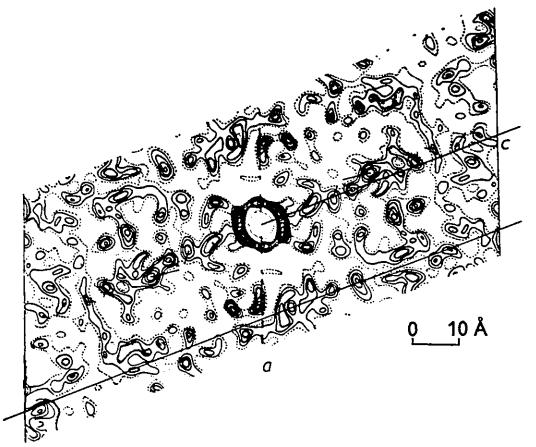

Fig. 5. The complete central section $y = 0$ of the vector map, obtained by repeating section given by Bragg *et al.* (1950) about the dyad axis. On it lines have been drawn, as in Fig. 4, section $y = 0$.

section published a year later by Bragg, Kendrew & Perutz (1950). As in the previous discussions, we indicate the positions of the vector rods of the (a) set by indicating the positions of their axes in various sections. Thus for the central section normal to the direction of the rods, the section normal to a, we have a hexagonal network indicating the points at which the axes of the rods pierce the section. On the ($a\,b$) central section and the ($a\,c$) sections, lines indicate the axes of vector rods.

Scrutinizing these sections, our attention is straightway riveted by two outstanding features, as we have earlier pointed out (Wrinch, 1952*a*, *b*). The first is 'the 5 Å shell' with the description of which Perutz begins his account of the map, a region of notably high vector density at 4–6 Å from and completely surrounding the origin, as we see in the sections 0–5 as well as in the remaining two central sections. Within, this shell is bounded by a broken contour, indicating that here the vector density has a value equal to the average for the unit cell.† Just inside the shell there is,

* The author is very greatly indebted to Dr Perutz for the loan of the Hollerith sheets giving this three-dimensional vector map in its entirety, in October 1951. In this preliminary examination of the vector map, only the published sections of the map are discussed.

† Perutz's vector function depicted in Figs. 4 and 5 is the Fourier transform of his relative intensities, taking the intensity at the origin to be zero. The actual vector function is therefore a linear function of this vector function. When Perutz's vector function takes zero values, as shown by the broken contours in the map, the actual vector function takes its average value for the complete unit cell. When it takes positive values, the actual vector function has higher-than-

therefore, a region of lower-than-average density which begins at about 3 Å from the origin, if we may judge from the section in Fig. 5 (on which alone the onset of the region is marked). This 'low density' shell, at 3–4 Å from and completely surrounding the origin, is the second striking feature of the vector map. In studies of the vector map, in and for itself, without presuppositions, which have the objective of eliciting from it direct indications regarding the nature of the structures in the crystal, the interpretation of these two features naturally takes the center of the stage from the outset of the enquiry (Wrinch, 1952*a*, *b*). In the view of the writer, there is little doubt that any discussion of the map which neglects to give a specific interpretation to these two features will necessarily result in conclusions which are incorrect. However, we will first proceed merely to study the nature of the vector distribution in the regions which should be occupied by the vector rods, paying as little attention to these two features as possible. Since the vector rods supposedly lying along the *a*-axis actually intersect both the low-density shell and the high-density shell, we have then to confine our attention, for the time being, to the case which can be made out for the presence in the vector map of the (*a*) and (*b*) sets of vector rods, excluding the central rods.

We may begin with the sections normal to the dyad axis. Since the metric of the network of the (*a*) set of rods is $b/6$, axes of the rods will lie only on sections $0, \pm5, \pm10, \pm15, \pm25, 30$ of the set of sections at 60ths of *b*. Accordingly, we see on the sections of Figs. 4 and 5 only five axes, which include the *a*-axis of the central rod to be discussed later. Taking the rods in order of increasing distance from the central rod, we begin with two sets at $b/6$. Axes of the rods I lie at $z'/c \sin\beta = \pm0{\cdot}18$, $60y/b = \pm5$, as indicated on map 5: axes of the rods I′ lie at $z = 0$, $60y/b = \pm10$, as indicated on map 10. We remark that the two rods of set I′ belong also to the (*b*) set of rods shown in Fig. 2. The other four non-central rods of the (*b*) set may be regarded as the I set somewhat displaced, with axes now at $z'/c \sin\beta = \pm1/6$, $60y/b = \pm7$. Next there is set II at $b/3/6$ from the central rod with axes along $z'/c \sin\beta = \pm0{\cdot}36$, $y = 0$, as indicated on map 0 (in Figs. 5 and 4). Finally, there is the set III at $2b/6$ from the central rod, with axes at $z'/c \sin\beta = \pm0{\cdot}36$, $60y/b = \pm10$, as indicated on map 10. Supplementary information concerning the I′ set (and the central rod) is given by the central (*a b*) section. Supplementary information concerning all of these rods, and the only information regarding all the remaining rods of the (*a*) set, is contained in the central section normal to *a*.

If the diameters of the supposed rods in the crystal are even as large as (say) 5 Å, the vector rods with radius 5 Å or more will cut each and every section shown; those with axes on 0 will cut at least the maps 1, 2, 3 and 4, those with axes on map 5 will cut at least the maps 1–9: those with axes on map 10 will cut at least the maps shown in the figure from 6 onwards. But how is it possible, in these sections, to make out any clear-cut case in favor of rod-like distributions to correspond to any of these four non-central rods?

When we look for the vector rod I whose axis lies on the line $z/c = 0{\cdot}18$ on section 5, we see a high-density mass on this line but only near the center of the section, and as much can be claimed on sections 6 and 7; but it is surely impossible to claim any general high density distribution about this line in sections 4 or 3 or 2 or 1. For the (*b*) set, the rod is displaced so that its axis lies along the line $z/c = 1/6$ on map 7. Here and on adjoining sections the concentration of peaks on or near this line is perhaps a little more convincing. But again the many regions of below-average density make the case in favor of the presence of the rod very weak. If we look for evidence of the rod I′, belonging to both the (*a*) and (*b*) sets, with its axis along the line $z = 0$ on map 10, we see some high-density regions but large intervals of below-average density between. Examining the adjoining maps 11 and 12, no confirmation of the presence of the rod appears. There remain only two other axes on this series of sections. One is the axis of rod II along the line $z/c = 0{\cdot}36$ on the central section shown in Fig. 5. On and about this line we see that any high-density regions that are present are very much interrupted, that there are, in fact, many regions of below-average density. Studying the same line in the sections on either side of the central section, i.e. in the identical sections $60y/b = \pm1$, $60y/b = \pm2$, *et seq.*, we must surely conclude that any idea that we can trace the imprint of this vector rod has to be abandoned. Finally, we look for the rod III with its axis along the line $z/c = 0{\cdot}36$ on map 10. Scrutinizing the vector-density distribution about this line we see only a region of predominantly below-average density, interspersed with a few regions which are slightly above-average in density. The hypothesis that there is a vector rod about this line receives little support in this section, still less in the adjoining sections. We therefore have no choice but to regard the case in favor of the presence of non-central vector rods of the (*a*) set or of the (*b*) set as extremely frail, so far as the sections normal to the dyad axis are concerned.

Turning to the two remaining sections, the central (*a b*) section and the central section normal to *a*, there seems little chance of bolstering it. Thus, looking at the central (*a b*) section, apart from the central rod lying along the lines $y = 0$ and $\frac{1}{2}b$, there is only the I′ rod about which any information can be gleaned. Its axis lies along the line $y/b = 1/6$—a line already studied on the section $60y/b = 10$—and continues

average values; when it takes negative values, the actual vector function has lower-than-average values. The zero level on the map thus is in no sense an arbitrary level, as Perutz (1949) asserts: it has a direct and important physical significance. These aspects of the vector map are discussed more fully elsewhere (Wrinch, 1952*a*, *b*, also unpublished work).

along the line $y/b = 1/3$ about which we have no previous information. But this new information amounts only to the observation that the vector density on and about this line is predominantly below-average. About the line already studied there is in this section little to confirm the presence of the vector rod. However, interestingly enough, we get the definite impression that the regions of high density which undoubtedly occur on the line near the center on either side, as we saw in map 10, belong to a system of widely spread high-density regions which fill much of the space at, say, 9½–15 Å from the origin. Thus, on these two central sections, we have one and the same impression: that much of this region, in very many different directions from the origin, is above-average in density. Going over the maps 0–12 once again, we find regions of high vector density within a spherical shell extending from, say, 9½ to 15 Å in every single section.

It remains only to study specifically the vector-density distribution in the central section normal to the a-axis on and near the whole set of points at which axes of the (a) set of vector rods cut this section, as indicated by the hexagonal network drawn on part of this section, and to make a corresponding study for the points for the (b) set. We remark that most of the (a) set of points fall in or very near regions of below-average density. The only points of the (a) set which lie in or very near regions of fairly high vector density are the points for rods II, namely $y = 0$, $z'/c \sin\beta = \pm 0{\cdot}36$, and for rods I, namely $y/b = \pm 5/60$, $z'/c \sin\beta = \pm 0{\cdot}18$. It is interesting to notice that the situation is somewhat improved when these rods I which emerge from the Bragg–Howells–Perutz structure are restored to their original positions in the (b) set with axes through the point $y/b = \pm 7/60$, $z'/c \sin\beta = \pm 1/6$. That the points for the remaining rods of the (b) set (called B rods by Perutz), which are also the rods I′ of the (a) set, namely $y/b = \pm 1/6$, $z' = 0$, lie in relatively low density regions is clear, as Perutz himself pointed out. His comment runs as follows: 'It seems surprising that no maximum appears in the positions where the rods B cross the section, but Fig. 19 shows that this rod actually has a minimum at $z = 0$' (Perutz's fig. 19 is obtained by superposing maps 9, 10 and 11 seen in Fig. 4). It may however, be suggested that the comment might more reasonably be to the effect that, so far as these sections are concerned, the evidence is that there are no B rods in the vector map and that the case for the B rods must be made, if at all, on evidence from other sections. Actually the only other evidence has already been studied.

We now conclude our unsuccessful search for evidence, in the sections of the three-dimensional vector map in Figs. 4 and 5, of the presence of the original (b) set of non-central vector rods claimed by Perutz and of the (a) set of non-central vector rods whose presence is required by the Bragg–Howells–Perutz structure. Before passing on to the second phase of the investigation, we may consider whether, with another choice of positions for vector rods a case for their presence could have been made out. A general survey of the sections suggests that this is not so, even with a change in the direction of the rods.

We may then turn to the remaining issue, namely the possible presence of vector rods actually on the a-axis. This further issue has to be discussed to complete our formal investigation of Perutz's claim and of the Bragg–Howells–Perutz structure, even though we now know in advance that little supporting evidence relating to any accompanying set of vector rods is to be found.

We see the imprint of the axis of the rod on the line $z = 0$ of the central (a c) section, $y = 0$, in Fig. 5 and on the line $y = 0$, continuing along the line $y = \frac{1}{2}b$ of the central (a b) section, $z' = 0$, in Fig. 4. We are now rapidly approaching the moment when the 3–4 Å low-density shell and the 4–6 Å high-density shell can no longer be disregarded since the supposed central rods cut directly across both of them. However, let us, for the time being, still look specifically for any other evidence there may be of the existence of the central rods, the last of the (a) and (b) sets to be considered.

Accordingly we examine the nature of the vector-density function along and in the neighborhood of the a-axis, looking for what Bragg *et al.* (1950) describe as 'a somewhat irregular but clearly marked rod of density ... through the origin and parallel to the a-axis, such as would be produced by the vectors between atoms of polypeptide chains running in this direction'.

Scrutinizing both the (a c) and (a b) central sections, we certainly do find numerous peaks on or near the a-axis. However, if any attempt is to be made to trace a vector rod of considerably more-than-average density the nature of the regions between and about the peaks has to be taken into account. We see in the (a b) central section and the (a c) sections through and near the origin that much of the territory about the a-axis, and some of the territory actually crossing it, is negative, indicating that the vector function there has values which are not merely lower than on any of the peaks but values which are below the average value for the whole crystal. In these circumstances, is it possible to claim the existence of central vector rods along the a-axis? Certainly the case for making this claim is very frail.

Postponing the final answer to this question, we may now take into consideration the fact that it is not merely any vector rod which is being looked for; in view of the 5 Å periodicity characterizing the postulated rod-like polypeptide chains, we are looking specifically for a rod bearing some manifestation of this periodicity, i.e. for some signs of a 5 Å periodicity along the a-axis and only along the a-axis.

Looking now at the high-density regions along the a-axis in more detail, we study first the four peaks within a single complex, marked a by Perutz on maps, 0, 1, and on the (a b) section. We see that they lie at,

say, 11·3, 17·2, 21·8 and 26·3 Å from the origin, agreeing only very roughly with Perutz's claim (1949, pp. 488–9) that they lie at 5 Å intervals. However, let us assume for the moment that these *a*-peaks may be regarded as vector interactions between pairs of atoms in the postulated rod-like polypeptide chains at distances apart corresponding to 2, 3, 4 and 5 times the basic repeat. We also see that this succession of peaks at, very roughly, 5 Å apart, continues thereafter, to correspond, we have to assume, though only very roughly, to vector interactions of pairs of atoms at 6, 7, ... times 5 Å apart. It should, however, be pointed out that there are at least two further features which challenge the correctness of this assumption. The heights of the peaks, even in the *a*-group, do not decrease monotonically to correspond to the necessarily decreasing numbers of pairs of atoms at distances apart corresponding to increasing multiples of the basic distance. Further, there are the peaks spreading around the origin in a large arc from the *a*-peak at about 11·3 Å from the origin (cf. Fig. 5) evidently forming, as it seems to the writer, part of the system of widely spread high-density regions filling much of the space, say 9½–15 Å from the origin, which we have already noticed in all the other sections. We are not looking for peaks spread in an arc around the origin. These peaks, marked *b* by Perutz (cf. map 0 in Fig. 4), constitute an unwanted feature.

4. The nature of the vector map in the neighborhood of the origin

It remains only to consider the manifestation of the supposed polypeptide chains with their 5 Å periodicity, which is to be expected in the vector map near the origin. It may be described as follows: a vector function with a pronouncedly uniaxial character—with respect to the *a*-axis—even very close to the origin, which develops, at about 5 Å from the origin, on or very near the *a*-axis, a well localized peak, somewhat higher, though not grossly higher, than the other peaks on the *a*-axis already discussed.

It is at this point that we can no longer exclude from consideration the features which dominate the experimental vector map in the neighborhood of the origin, the 3–4 Å low-density shell and the 4–6 Å high-density shell with its intricate morphology mapped by the contour surfaces. They are excluded from discussion by Perutz, who confines himself to a reference to 'the 5 Å vector peak along the chain direction' and in his 'idealized' vector rods, reproduced in Fig. 2, shows only this feature with the rest of the 5 Å shell which is found in his experimental vector map replaced by an essentially cylindrical distribution.

Looking carefully at the sections 0–7 and the two other central sections of the vector map in Fig. 4 we see not only the S_1 peak, to which Perutz does refer, but also four other pairs, the S_2 and the S pairs and the two S_3 pairs, so named by Perutz himself. We see, around the origin in the central section normal to the 'chain direction', a 4–6 Å ring of high density, a ring which is very similar to the 4–6 Å ring of high density seen in the other two central sections which both contain the 'chain direction'. Above all, we see the shell enclosing these five pairs of peaks and itself completely surrounding the origin, and the inner low-density region, also a shell completely surrounding the origin. In S_1 we have evidence of many pairs of atoms at about 5 Å apart, set to one another in directions not far from the *a*-direction. However, in the shell we have evidence of a relatively large numbers of pairs of atoms at 4–6 Å apart, set to one another not only in these directions but in all directions, numbers sufficiently large to account for the whole of this origin-circumscribing region being positive, i.e. of density above the average for the crystal. And in the 3–4 Å region we have, correspondingly, evidence of relatively small numbers of pairs of atoms at 3–4 Å apart, set to one another in all directions, numbers sufficiently small to account for the whole of this origin-circumscribing region being negative. Evidently, then, it may be claimed that the expected signs of the presence of the chains with their 5 Å repeat, in the *a*-direction and only in the *a*-direction, have failed to materialize.

The situation may, then, be summed up very simply. Even when the experimental vector map is studied only from the origin up to about 6 Å, the following information can be gleaned. By and large, the local architecture of the individual structures in the crystal is such that atoms at distances apart covered by this range of lengths are not arranged uniaxially with respect to any direction, nor for that matter biaxially. On the contrary, they are arranged in an essentially three-dimensional manner. Such a range of lengths covers nearest neighbors in covalently bonded structures, also second nearest, third nearest and even more remote neighbors; it further covers pairs of atoms held in a hydrogen bridge, and indeed first, second and some third nearest neighbors in any hydrogen-bridged arrays of atoms which may be present in the crystal. With an essentially three-dimensional distribution of the vectors between atoms and their neighbors within, say, a 6 Å sphere, and, indeed, no uniaxial character in the vector map as a whole, we can finally conclude that there is no confirmation of the hypothesis of rod-like polypeptide chains in the crystal.

5. Conclusions

Our limited objectives in this communication have already been defined. They relate to the existence of the vector rods claimed by Perutz in 1949 and to the light thrown by the vector maps on the possibility that horse hemoglobin has the Bragg–Howells–Perutz structure or any similar structure comprising parallel polypeptide chains.

Regarding the first issue and part of the second and third issues, conclusions may now be drawn. There is

no case for the existence of Perutz's set of vector rods, or of the (*a*) set of vector rods, or of any set of parallel vector rods, either in the vector projections first discussed or in the three-dimensional vector map which has now been examined in some detail, especially in the neighborhood of the origin.

A final conclusion regarding the second and third issues requires a decision on one further point. Claiming the non-existence of the vector rods emerging from the Bragg–Howells–Perutz structure or any similar structure, can we proceed to claim that all these structures for horse hemoglobin are to be rejected?

Before answering this question, one other must be posed. Less than half the volume of this heavily hydrated protein crystal is protein (Boyes-Watson *et al.*, 1947). Is it, then, possible to take the line that the rod-like polypeptide chains may be present and yet fail to indicate their presence? Can we perhaps say that the presence of such structures, while not confirmed, is not disproved? To maintain this viewpoint, we would have to advance a certain hypothesis about the distribution of the additional vectors brought in when the water complement is considered. These additional vectors comprise 'water–water' vectors between atoms of the water molecules and 'water–protein' vectors between an atom of a water molecule and an atom in one of the postulated polypeptide chains. The hypothesis which has to be advanced is that these additional vectors are of such a nature that, superposed on the rod-like distribution of protein–protein vectors, an essentially three-dimensional distribution, with no uniaxial quality in any direction, results, in particular in the 3–4 Å and 4–6 Å ranges. Assuming that the protein structures which co-opt the water molecules to facilitate crystallization comprise sets of parallel rod-like chains, there is no reason to suppose that the water–protein vectors would yield a distribution of this kind. Regarding the water–water vectors, an accentuation of the rod-like quality of the vector distribution or, at best, an essentially three-dimensional distribution would be expected. That the superposition of the additional vectors should change vector rods along the *a*-direction or any other direction into a high-density shell in the range 4–6 Å and a low-density shell in the range 3–4 Å is an untenable viewpoint.

It seems, therefore, that it is not possible to take the line that there are parallel polypeptide chains in the crystal and that the absence of the vector rods near the origin can be explained in terms of protein–water and water–water vectors. In other words, the nature of the vector-density distributions, as seen in the vector-map sections shown in Figs. 4 and 5 and the vector projections in Figs. 3 and 4, indicates that there are no sets of parallel rod-like structures in the methemoglobin crystal, in the *a*-direction or, indeed, in any direction. It follows that the successful interpretation of the vector map is not a question of a successful choice of a direction for a set of parallel rod-like polypeptide chains (Perutz, 1949), a successful choice of the number and positions of the chains in such a set (Perutz, 1949; Bragg *et al.*, 1952), with the only remaining issue the formulation of configurations which the polypeptide chains may 'reasonably' be expected to assume (Bragg *et al.*, 1950) and the consequent successful choice of one of them (Wrinch, 1953).

We are then faced with the fact that, in the case of horse hemoglobin, the classical theory that a protein entity is made up of a set of parallel rod-like polypeptide chains has to be abandoned. The next communication in this series will take a different tack and will further develop the attempt to elicit from the vector map, particularly in the neighborhood of the origin, direct indications regarding the nature of the structures in the horse methemoglobin crystal (Wrinch, 1952*a*, *b*, 1953).

References

Boyes-Watson, J., Davidson, E. & Perutz, M. F. (1947). *Proc. Roy. Soc.* A, **191**, 83.

Bragg, W. L., Howells, E. R. & Perutz, M. F. (1952). *Acta Cryst.* **5**, 136.

Bragg, W. L., Kendrew, J. C. & Perutz, M. F. (1950). *Proc. Roy. Soc.* A, **203**, 321.

Crowfoot, D. (1941). *Chem. Rev.* **28**, 215.

Perutz, M. F. (1949). *Proc. Roy. Soc.* A, **195**, 474.

Wrinch, D. (1949). Unpublished work.

Wrinch, D. (1952*a*). *J. Chem. Phys.* **20**, 1051.

Wrinch, D. (1952*b*). *J. Chem. Phys.* **20**, 1332.

Wrinch, D. (1953). *Acta Cryst.* **6**, 562.